

## OPEN

# A novel animal model of primary blast lung injury and its pathological changes in mice

Xiang-Yan Meng, PhD, Qian-Ying Lu, PhD, Jian-Feng Zhang, BS, Jun-Feng Li, BS, Ming-Yu Shi, BS, Si-Yu Huang, BS, Si-Fan Yu, BE, Yan-Mei Zhao, PhD, and Hao-Jun Fan, PhD, Tianjin, China

**BACKGROUND:** Primary blast lung injury (PBLI) is a major cause of death in military conflict and terrorist attacks on civilian populations. However, the mechanisms of PBLI are not well understood, and a standardized animal model is urgently needed. This study aimed to establish an animal model of PBLI for laboratory study.

**METHODS:** The animal model of PBLI was established using a self-made mini shock tube simulation device. In brief, mice were randomly divided into two groups: the control group and the model group, the model group were suffered 0.5 bar shock pressures. Mice were sacrificed at 2 hours, 4 hours, 6 hours, 12 hours, and 24 hours after injury. Lung tissue gross observation, hematoxylin and eosin staining and lung pathology scoring were performed to evaluated lung tissue damage. Evans blue dye leakage and bronchoalveolar lavage fluid examination were performed to evaluated pulmonary edema. The relative expression levels of inflammation factors were measured by real-time quantitative polymerase chain reaction and Western blotting analysis. The release of neutrophil extracellular traps was observed by immunofluorescence stain.

**RESULTS:** In the model group, the gross observation and hematoxylin and eosin staining assay showed the inflammatory cell infiltration, intra-alveolar hemorrhage, and damaged lung tissue structure. The Evans blue dye and bronchoalveolar lavage fluid examination revealed that the lung tissue permeability and edema was significantly increased after injury. Real-time quantitative polymerase chain reaction and Western blotting assays showed that IL-1 $\beta$ , IL-6, TNF- $\alpha$  were upregulated in the model group. Immunofluorescence assay showed that the level of neutrophil extracellular traps in the lung tissue increased significantly in the model group.

**CONCLUSION:** The self-made mini shock tube simulation device can be used to establish the animal model of PBLI successfully. Pathological changes of PBLI mice were characterized by mechanical damage and inflammatory response in lung tissue. (*J Trauma Acute Care Surg.* 2022;93: 530–537. Copyright © 2022 The Author(s). Published by Wolters Kluwer Health, Inc. on behalf of the American Association for the Surgery of Trauma.)

**KEY WORDS:** Lung; blast injury; animal model; shock wave; inflammation.

Accidental explosion are common in various fields, such as military, industry, and daily life. Blast injuries are the most common fatal injuries sustained during military actions, terrorist attacks, and peacetime accidents.<sup>1</sup> Research from WHO staff suggests that blast injuries account for 79% of combat-related injuries.<sup>1</sup> In a review by Mackenzie and Tunnicliffe,<sup>2</sup> among the 517 blast injured patients admitted to intensive care at the

University Hospital of Birmingham between July 1, 2008, and January 15, 2010, 95 (18.4%) died before receiving treatment and 17 died during subsequent treatment. In the battlefield and terrorist attacks, among the blast injuries caused by explosive weapons, brain, ear, limbs, chest, blood vessels are mainly damaged, among which chest trauma accounts for a large proportion with the highest morbidity and mortality.<sup>3</sup> Chest trauma mainly includes penetrating injury, blunt trauma, and blast injury. The lung in the chest is the most important target organ in blast injury because of its air-containing, which is called blast lung injury (BLI).

The pattern of blast injury could be divided into five grades: primary, secondary, tertiary, quaternary, and quinary blast injuries. Damage caused only by the blast wave was defined as primary blast injury.<sup>4</sup> Primary BLI (PBLI) is also defined as “radiological and clinical evidence of acute lung injury occurring within 12 hours of exposure and not due to secondary or tertiary injury.” In the war of Afghanistan, PBLI was identified in 6% to 11% of military casualties surviving to reach a field hospital.<sup>5</sup> The incidence of PBLI can reach almost 80% in blast exposed nonsurvivors.<sup>6</sup> About 94% of severe casualties in the Madrid train bombings suffered PBLI.<sup>7</sup> Therefore, it is very important to study the pathogenesis and treatment of PBLI and reduce casualties in the war. Although a vast amount of blast injury animal researches have been undertaken since the Second World War, the laboratory animal model that could fully simulate PBLI remains absent.

Submitted: October 27, 2021, Revised: January 27, 2022, Accepted: January 31, 2022, Published online: March 7, 2022.

From the Institute of Disaster and Emergency Medicine (X.-Y.M., Q.-Y.L., J.-F.Z., J.-F.L., M.-Y.S., S.-Y.H., S.-F.Y., Y.-M.Z., H.-J.F.), Tianjin University; and Tianjin Key Laboratory of Disaster Medicine Technology (X.-Y.M., Q.-Y.L., J.-F.Z., J.-F.L., M.-Y.S., S.-Y.H., S.-F.Y., Y.-M.Z., H.-J.F.), Tianjin, China.

X.-Y.M., Q.-Y.L., and J.-F.Z. contributed equally to this work.

Supplemental digital content is available for this article. Direct URL citations appear in the printed text, and links to the digital files are provided in the HTML text of this article on the journal's Web site ([www.jtrauma.com](http://www.jtrauma.com)).

Address for reprints: Yan-Mei Zhao, PhD, Tianjin University, No. 92, Weijin Road, Nankai District, Tianjin; email: [zhaoyanmei@126.com](mailto:zhaoyanmei@126.com); Hao-Jun Fan, PhD; email: [haojunfan86@163.com](mailto:haojunfan86@163.com).

This is an open-access article distributed under the terms of the Creative Commons Attribution-Non Commercial-No Derivatives License 4.0 (CCBY-NC-ND), where it is permissible to download and share the work provided it is properly cited. The work cannot be changed in any way or used commercially without permission from the journal.

DOI: 10.1097/TA.00000000000003571

Shock wave is an important cause of blast injury and can induce complex damage to multiple systems and organs owing to instantaneous overpressure. In this study, we aim to design a mini shock tube simulation device for the establishment of PBLI animal model suitable for laboratory study and explore the complex pathophysiological changes caused by blast injury to the lungs in mice.

## MATERIALS AND METHODS

### The Self-Made Mini Shock Tube Simulation Device

In this study, the mouse PBLI model was induced by a self-made mini shock tube simulation device. The device consists of five parts: compression chamber, release chamber, pricking device, pressure sensor, and computer control system (Fig. 1). This device weighs about 80 kg. Both compression chamber and release chamber are vertical steel tubes with a diameter of 400 mm and a height of 200 mm and 500 mm, respectively. The two chambers are separated by multilevel tin foils in the middle and secured by lifting ring bolts, where a damaging shock wave is generated with peak pressures ranging from 0 bar to 5 bar. The device has two pressure sensors: one is located in the cylinder wall of the compression chamber and is used to measure the preexplosion pressure in the compression chamber; another is located in the shock wave release port of the release chamber and measures the peak pressure of the shock wave actually applied to the experimental animals. The two sensors are both connected to a computer control system to record and display real-time pressure in both chambers at a frequency of 200 Hz/s. A special rubber plate with holes (the diameter of the holes is 20 mm) is fixed on the upper part of the release chamber, which is also seen as a platform for animal placement. The pricking device is installed in the middle of the release chamber. The computer control system can set the data of burst pressure and display the real-time change of air pressure in the two chambers, store and transmit the relevant data. The compression chamber is connected with an air compressor. The compressed air is injected into the compression chamber through the air compressor when the control system is turned on. When the pressure-setting value is reached, the pricking device pierces the aluminum film and produces instantaneous shock wave. Scatter plots of the peak pressure were drawn using origin software version 9.0 and fitted by a linear line to determine the shock-wave loading trend.

### Animals and Mouse PBLI Model

Male C57BL/6 mice, aged 6 weeks to 8 weeks and weighing 18 g to 24 g were purchased from Beijing Vital River Laboratory Animal Technology Co., Ltd. (Beijing, China). Animals were housed four to five per cage at 22°C with a 12-hour light/dark cycle, and free access to food and water. Animal welfare and experimental design were approved by the Institutional Animal Care and Use Committee of Yi Shengyuan Gene Technology (Tianjin) (YSY-DWLL-2021013).

Forty mice were randomly divided into four groups (n = 10 for each group). After administering anesthesia, mice were placed in a prone position on the rubber plate with the chest directly above the hole. The mice were suffering from 0.5 bar, 1 bar, 1.5 bar, or 2 bar shock pressures, respectively. Physiolog-

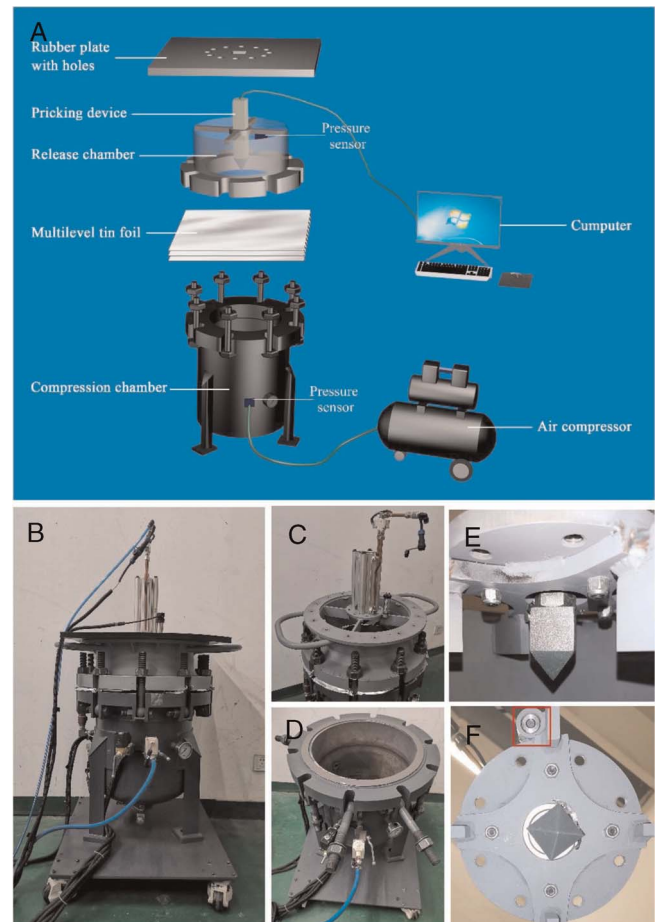


**Figure 1.** The self-made mini shock tube simulation device. (A) Model diagram of the device. The device consists of five parts: compression chamber, release chamber, pricking device, pressure sensor and computer control system. Both the compression chamber and the release chamber are respectively vertical steel tubes and are separated by multilevel tin foils in the middle. The compression chamber is connected with an air compressor. The compressed air is injected into the compression chamber through the air compressor when the control system is turned on. When the pressure-setting value is reached, the pricking device pierces the aluminum film and produces instantaneous shock wave. The shock wave generated by the device ranges from 0 to 2 bar. (B–F) Photos of the device. (B) Shock tube main body. (C) Release chamber. (D) Compression chamber. (E) Pricking device. (F) Pressure sensor.

ical status and survival were observed every 2 hours for the first day after injury. From the second day after the injury, mice survival was observed once a day.

According to the results of survival study above, 0.5 bar was finally selected as the injury pressure. Another 48 mice were randomly divided into the control group and the model group. The model group suffered 0.5 bar shock pressures, and the control group was treated similarly but without exposure to shock wave. The lungs of the mice in each group were harvest and weighted at 2 hours, 4 hours, 6 hours, 12 hours, and 24 hours after injury (n = 8 for each group).

This study conforms with the ARRIVE guidelines and a complete checklist has been uploaded as Supplemental Digital Content (SDC 1, <http://links.lww.com/TA/C388>).

## Hematoxylin and Eosin Staining and Lung Pathology Scoring

The right lung of mice was harvest and placed in 4% paraformaldehyde fix solution. Paraffin embedding and slices were used for hematoxylin and eosin (H&E) staining. The lung pathological injury was scored according to the H&E results of lung tissue sections and lung pathology scoring standard.<sup>8</sup> Pathological injury was scored according to the following variables: alveolar and interstitial inflammation, alveolar and interstitial hemorrhage, edema, alveolar fusion, alveolar septal thickening. The severity of each of the seven indicators is graded as follows: no damage was graded as 0 point, damage with 25% was 1 point, damage with 50% was 2 points, damage with 75% was 3 points, and diffuse damage was 4 points. The highest score is 28 points and the lowest is 0 point.

## Lung Vascular Permeability Assay

Lung vascular permeability was evaluated by measuring Evans blue dye (EBD) leakage. In brief, 4% EBD (5 mL/kg) was injected intravenously at each time point after blast injury. The mice were sacrificed 2 hours after injection. A small incision was made in the left atrium with ophthalmic scissors, and phosphate buffer solution (PBS) containing heparin sodium perfusion through the right ventricle was performed followed by a 20-mL rinse. Then the lungs were removed and placed into 1 mL Dimethylformamide. After incubated at 60°C for 24 hours, the tissue were centrifuged at 4,000 rpm for 10 minutes. The supernatant was collected and the absorbance was detected at 620 nm. According to the standard curve, the content of EBD in lung tissue was calculated.

## Bronchoalveolar Lavage Fluid Examination

After sacrificed, the trachea of the mice was exposed. A small incision was made below the thyroid cartilage and an 18-G endotracheal intubation was inserted, ligated and fixed. Mice trachea was lavaged with 0.4 mL PBS each time, repeated for three times, and collected bronchoalveolar lavage fluid (BALF) solution. Then the BALF was centrifuged at 6,000 rpm for 15 minutes, the supernatant was collected and the protein concentration was detected. After washing twice with PBS, the pre-

cipitation was mixed with 2% glacial acetic acid, the total number of leukocyte was counted under a microscope. Leukocyte cell smears were prepared, and the total leukocyte were counted under a microscope after staining with Giemsa solution.

## Real-Time qPCR

The total RNA was extracted from the lung tissues using the TRIzol reagent (Invitrogen, USA), the concentration and purity of RNA were detected using NanoDrop One Microvolume UV-Vis spectrophotometer. RNA reverse transcription was performed using PrimeScript RT reagent Kit (TaKaRa, Japan) and Mastercycler pro PCR instrument (Eppendorf, GER). Real-time quantitative polymerase chain reaction (qPCR) was performed using HieffTM qPCR SYBR Green Master Mix (Yeasen, China) and LightCycle 96 instrument (Roche, Swiss). Gene expression was analyzed by LightCycle 96 software. The expression level was normalized to that of  $\beta$ -actin, and was calculated using the  $2^{-\Delta\Delta Ct}$  method. The primer sequences and running program in real-time qPCR are shown in Table 1.

## Western Blot

The lung tissues were lysed by lysis buffer. After incubating on ice, the supernatant was obtained by centrifugation at 12,000 rpm for 15 minutes. The protein concentration was measured by BCA assay. The protein was added to SDS-PAGE sample loading buffer, boiled and denatured for 10 minutes. After SDS-PAGE gel electrophoresis, the protein sample was transferred to the PVDF membrane and sealed with 5% skimmed milk for 2 hours. Then the appropriate primary antibody IL-1 $\beta$  (1:1000; cat. no. ab205924; Abcam, Cambridge, UK), IL-6 (1:1000; cat. no. 12912; Cell Signaling Technology, Boston, MA), TNF- $\alpha$  (1:1000; cat. no. ab215188; Abcam), Myeloperoxidase (MPO) (1:500; cat. no. sc-390109; Santa Cruz Biotechnology, Inc., Dallas, TX),  $\beta$ -actin (1:5000; cat. no. bs-0061R; Bioss, Beijing, China) were added and incubated overnight at 4°C. Then, the membrane was washed three times with tris buffered saline (TBS) with Tween (TBST), and a horseradish peroxidase-labeled antimouse secondary antibody (1:2000; cat. no. CW0102; Cowin Biosciences, Jiangsu, China), antirabbit secondary antibody (1:5000; cat. no. EF0002; Sparkjade, Shandong, China) were incubated for 1 hour at room temperature. The membrane was washed three times with TBST. Proteins were visualized using an ECL hypersensitive chemiluminescence kit (Sparkjade, cat. no. ED0016-B; Shandong, China)

**TABLE 1.** Sequence of Primers and Real-Time qPCR Running Program

Gene	Primer	Sequence of Primers	Real-Time qPCR Running Program
IL-1 $\beta$	Forward	TGCCACCTTTTGACAGTGATG	(1) Preincubation > 95°C for 5 min (2) Amplification (50 cycles) > 95°C for 10 s > 56°C for 20 s > 72°C for 20 s (3) Melting > 95°C for 10 s > 65°C for 60 s > 97°C for 1 s (4) Cooling 37°C for 30 s
	Reverse	AAGTCCACGGGAAAGACAC	
IL-6	Forward	TAGTCCTTCTACCCCAATTTC	
	Reverse	TTGGTCCTTAGCCACTCCTTC	
TNF- $\alpha$	Forward	CATCTTCTAAAATTCGAGTGACAA	
	Reverse	TGGGAGTAGACAAGGTACAACCC	
$\beta$ -actin	Forward	AGTGTGACGTTGACATCCGT	
	Reverse	GCAGCTCAGTAACAGTCCCG	

and a Tanon 5200 Full automatic chemiluminescence image analysis system (Tanon Science and Technology Co., Ltd, Shanghai, China).

### Immunofluorescence Staining

The lung tissues section was deparaffinized with xylene and dehydrated with ethanol gradient, and the antigens were repaired with 0.01 M citrate buffer (pH 6.0). After 30 minutes incubation with 0.1% Triton X-100, the tissues were sealed with 10% sheep serum for 30 minutes. Then the primary antibody, MPO (1:50; cat. no. sc-390109; Santa Cruz Biotechnology, Inc.), citH3 (1:50; cat. no. ab5103; Abcam) were incubated at 4°C overnight. After washing with PBS for three times, the fluorescent secondary antibody was added. Finally, the nuclei were stained by 4,6-diamino-2-phenyl indole (DAPI). All sections were analyzed under confocal microscopy.

### Statistical Analysis

Statistical analysis was performed using the Excel software V2019. All data were presented as mean ± SE; The homogeneity variance and one way ANOVA were applied to the whole sample study. The Kaplan–Meier method was used to evaluate the survival rates of the experimental animals, and a logarithmic survival curve was plotted.  $\chi^2$  Test was used to compare the survival rates among each group. All the statistical tests were two-tailed tests, with statistical significance defined as *p* less than 0.05.

## RESULTS

### Parameters of Shock Wave and Survival Rate of Animals

The self-made mini shock tube simulation device (Fig. 1) was used to establish the PBLI animal model. The peak pressure with a setting pressure of 0.5 bar, 1 bar, 1.5 bar and 2 bars is shown in Figure 2A. As a result, the peak pressure increases as the setting pressure increases.

Almost all mice in the four groups showed shallow breathing after the blast injuries. In the 1 bar, 1.5 bar, and 2 bar groups, some mice also showed a faint heartbeat. All animals remained alive in the 0.5 bar group. In the 1 bar group, two mice died in 24 hours after PBLI. And pulmonary hemorrhage was observed after dissection. All mice in the 1.5 bar group died within 24 hours (of which two had bleeding in the eyes). Lung tissue and thoracic cavity hemorrhage were observed after dissection. In the 2 bar group, eight mice died within 12 hours. No rib fractures were found in each group, and death occurred within 24 hours only. The survival rates in the 0.5 bar, 1 bar, 1.5 bar, and 2 bar groups were 100%, 80%, 0% and 20%, respectively (Fig. 2B).

### Gross Anatomy Observations of Lung Tissue

The lung tissue was generally observed after injury. A small area of hemorrhagic spots appeared in the pulmonary lobe of mice 4 hours after injury. Diffuse hemorrhagic spots formed 6 hours after injury, and the hemorrhagic lesions appeared dark red. The range of hemorrhagic spots decreased 12 hours after injury, and the color of the hemorrhagic lesion became lighter. The lungs were essentially normal approximately 24 hours after injury (Fig. 2C).

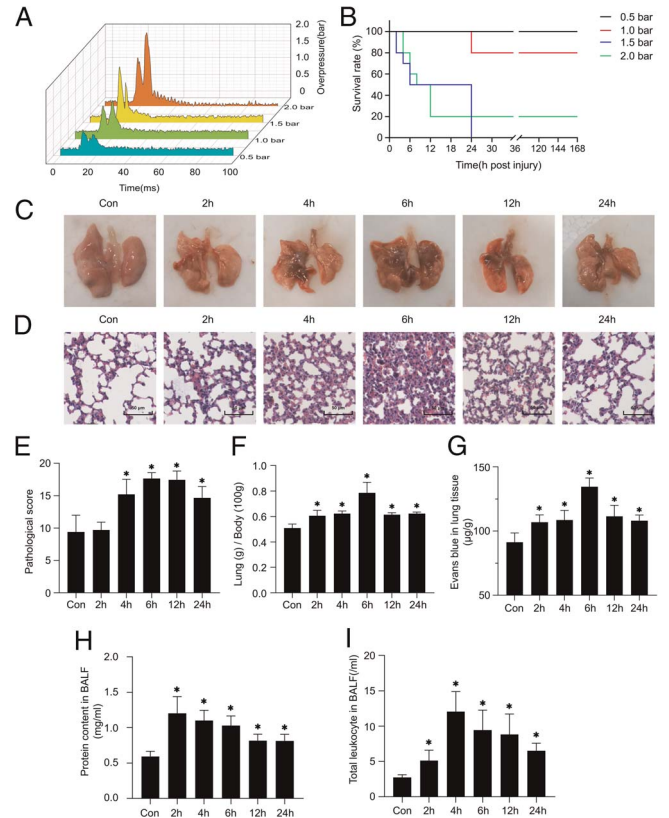


**Figure 2.** Lung tissue damage in mice after explosion. (A) Diagram of the peak pressure of shock wave generated by the device changing with time (0.5–2.0 bar). (B) Survival analysis of the animals with blast injuries at different shock wave pressure (0.5–2.0 bar). (C) Gross observation of lung tissue. (D–E) H&E staining and pathological scores of lung tissues. (F) The lung coefficient in each group. (G) EBD leakage test to detect pulmonary vascular injury. (H–I) Total protein concentration and leukocyte in BALF. Results are presented as mean ± SD. \**p* < 0.05.

### Pathological Results

Compared with the control group, the lung tissue in the model group was significantly damaged. Inflammatory cell infiltration into the alveolar compartment, intra-alveolar hemorrhage, thickening of lung alveolar septum, and lung tissue structure damaged were found in the model group. Two hours after injury, the alveolar septa were thickened and a few inflammatory cells were recruited. Four to 6 hours after injury, the alveolar structure of the lung is severely damaged, inflammatory cells and erythrocyte infiltrate into the alveolar cavity, the alveolar cavity is fused and reduced in volume. A large number of red blood cells remained in the alveolar cavity 12 hours after injury, indicating that there was still internal hemorrhage in the lung at this time. Twenty-four hours after injury, the levels of inflammatory cells and red blood cell infiltration were improved (Fig. 2D). According to the lung injury score, lung injury was significantly increased in the model group. Pathological scores increased significantly at 4 hours, and reached the peak at 6 hours to 12 hours. Compared with the control group, the score is still significantly higher 24 hours after injury (Fig. 2E).

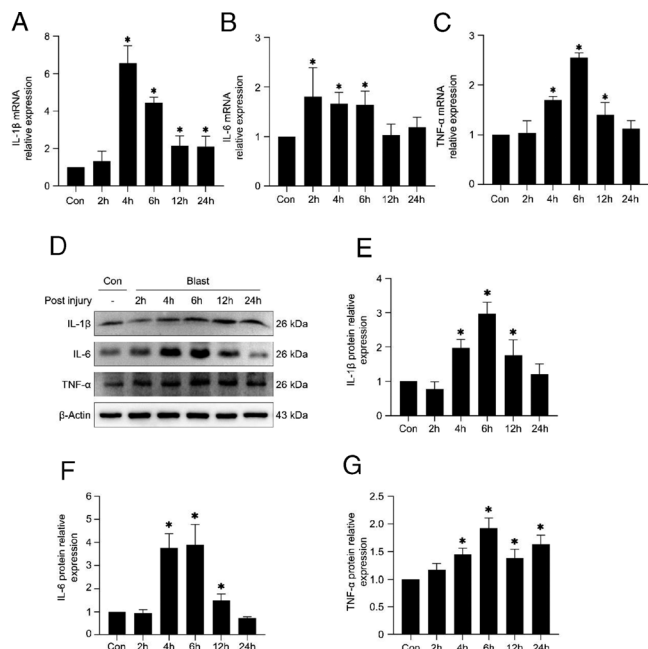


**Figure 3.** The expression of inflammation factors in the PBLI mice model. qRT-PCR and Western blotting analyses the IL-1β (A,D,E), IL-6 (B,D,F), and TNF-α (C,D,G) expression after injury at 2 hours, 4 hours, 6 hours, 12 hours, and 24 hours. Results are presented as mean ± SD. \**p* < 0.05.

### Lung Coefficient

Compared with the control group, the lung coefficient increased significantly 2 hours after injury and peaked at 6 hours. At 12 hours and 24 hours after injury, the lung coefficient was lower than that at 6 hours, but still significantly higher than that of the control group. These indicated that pulmonary edema persisted for at least 24 hours (Fig. 2F).

### Lung Vascular Permeability

The EBD assay showed that the dye leaked into the lung tissue, which indicated that the pulmonary blood vessels ruptured after PBLI. As shown in Figure 2G, increased vascular permeability was observed at model groups. Also, the level of EB in lung tissue reached the peak at 6 hours, which indicated that the diffuse vascular leakage in the lung tissue of the mice was highest at 6 hours after injury.

### Protein Content and Leukocyte Number in BALF

The total protein and cell content in BALF show the changes of permeability of pulmonary capillaries and alveolar epithelial cells. Compared with the control group, the total protein content in BALF increased significantly at model group (*p* < 0.05) after injury (Fig. 2H). As for the total cells number of leukocyte in BALF, it is increased significantly after injury and reached a peak at 2 hours (Fig. 2I).

### Inflammation Factors Expression

The expression of IL-1β, IL-6, and TNF-α was used to evaluate inflammation in the lung tissue after PBLI. The mRNA expression of IL-1β increased significantly and peaked at

4 hours after injury, then decreased gradually (Fig. 3A). The protein expression level of IL-1β started to increase at 4 hours and reached the peak at 6 hours after injury (Figs. 3D, E). At 2 hours to 6 hours after injury, IL-6 mRNA expression level significantly increased compared with that of the control group (Fig. 3B), the protein expression level of IL-6 increased at 4 hours to 12 hours and reached the peak at 6 hours after injury (Figs. 3D, F). As for TNF-α, the mRNA expression was significantly higher at 4 hours to 12 hours, and peaked at 6 hours after injury. Twenty-four hours after injury, the mRNA expression level of TNF-α basically returned to normal level (Fig. 3C); however, the protein expression level was still significantly increased (Figs. 3D, G).

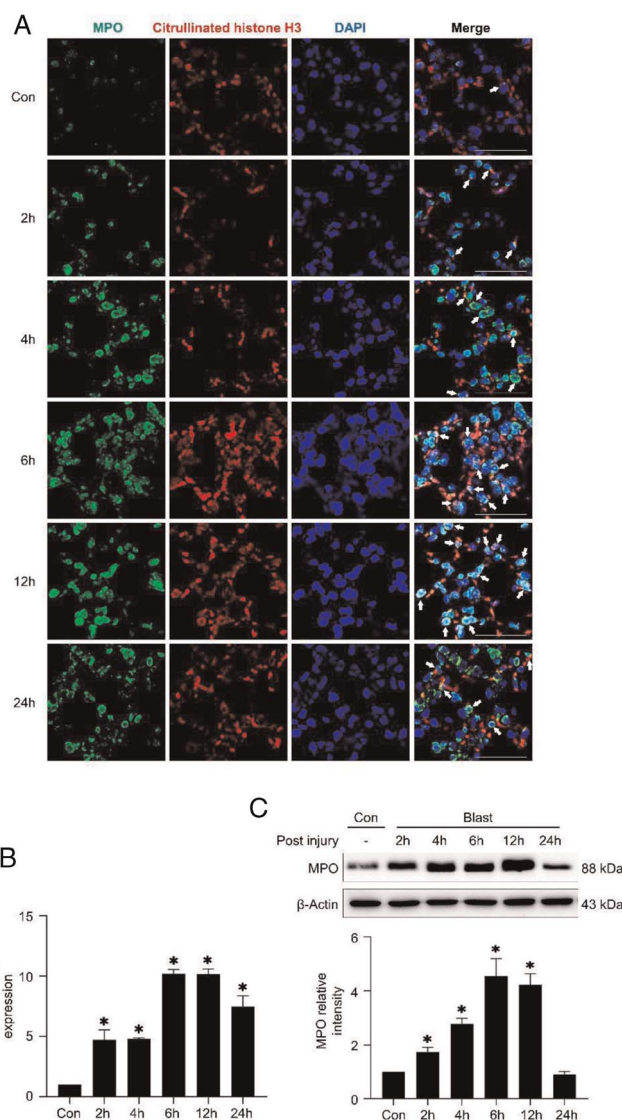


**Figure 4.** The level of NETs in lung tissue. (A,B) Immunofluorescence assay shows the level of NETs in the lung tissue after injury. Citrullinated histone H3 is stained red, Myeloperoxidase is stained green and DNA is stained blue. (C) Western blotting analyses the expression of MPO.

## The Level of Neutrophil Extracellular Traps in Lung Tissue

The level of neutrophil extracellular traps (NETs) was measured by immunofluorescence assay. As shown in Figure 4A, in confocal microscopy images, the colocalization of citrullinated histones H3 (red fluorescence), MPO (green fluorescence), and DAPI (blue fluorescence) is where the NETs are located. Compared with the control group, the level of NETs in the lung tissue increased significantly in the model group and reached the peak at 6 hours to 12 hours (Fig. 4B). MPO is a component of NETs, and its protein expression is highly correlated with the level of NETs.<sup>9</sup> The level of MPO in the lung tissues of mice in the model group was significantly increased at 2 hours to 12 hours after injury, and peaked at 6 hours, but there was no significant difference between the model group and the control group at 24 hours (Fig. 4C).

## CONCLUSION

Primary BLI is a major cause of death in military conflict and terrorist attacks on civilian populations. However, the detailed damage process and mechanisms of PBLI are not well understood. To study the complex pathophysiological changes of PBLI, a reproducible model is required to standardize outcomes and analyze interventions.

Yang et al. developed a type of real explosive device, in which a compression explosive column was used as the source of the open-field explosion. By this device, they established blast injury model in rats. Wu et al.<sup>10</sup> observed pathological changes in the rabbits caused by the blast wave, which caused by detonator explosion. The real-time signal was recorded by a pressure sensor attached to the rabbit's right chest. These modeling methods need to be performed outdoors in a wide area and have strict requirements on the site. In addition, it is necessary to protect the animal's body, otherwise it is easy to cause complex injuries instead of PBLI. These types of test also need higher expenses, lots of manpower, and material resources, and pathophysiological test is inconvenient to be performed at site.<sup>10,11</sup>

With the development of science and technology and the deepening of the research in this field, it was found that shock waves were generated mainly by detonating explosives outdoors and was the main factor causing blast injury. The researchers paid attention to shock tubes, the devices that could generate shock waves and tried to build the blast injury model caused by a single shock wave. By shock tubes, the injury induced by compressed air instead of explosive air, without heat and debris generation, with advantages of single injury, good repeatability and safety, and easy data collection. This kind of model is widely used at present.<sup>8,12,13</sup> Mishra et al.<sup>14</sup> developed a 9-in. square cross section, 6-m-long shock tube instrumented with pressure sensors. This shock tube could reproduce complex shock wave signature after a single shot was fired. Compared with commercially available shock tubes, most currently used in biological experiments have been modified to reduce their range or size to make them more suitable for laboratory environments. Even so, the shock tube is not very suitable for pulmonary study for placing horizontally. Tong et al.<sup>8</sup> self-designed a smaller shock tube stimulation device, which is placed vertically and induced blast injury by using compressed air to form a shock wave

produced by cracked an aluminum foil directed at a certain part of the mouse body.

Our device used in this study was modified from Tong's<sup>8</sup> shock tube simulation device in two main ways. First, a metallic firing pin was added in the device, which can pierce the aluminum foil directly when the burst pressure reaches at preset value. The multilayer aluminum foils were pierced by the computer-controlled pricking pin at preset value actively, instead of being cracked passively. This method will not be affected by the thickness of multilevel aluminum foils and is more accurate to reduce the error between the release pressure and the preset pressure. Second, mice were placed on a thick rubber plate with holes, allowing a specific body part of the mouse to be exposed to the shock wave, and the rest parts of body were isolated. Under the rubber plate, there is a pressure sensor that measure the real-time pressure record at the moment of blast. This can help us screen the experimental data that the actual burst pressure is consistent with the preset pressure. So, we have successfully developed a mini shock tube simulation device, which could induce PBLI in mice and is very suitable for indoor laboratory environment. Compared with previous devices, it has advantages of higher accuracy and smarter controls. The use of this device includes but is not limited to pulmonary experiments. We can change the exposed area of shock wave by replacing the animal fixing rubber plate. Also, through changing the exposed parts of animals, we can achieve the blast injury of different parts of animals, such as the whole body, intestine, ear, brain, limbs, and so on. In this way, our device can be used by researchers in orthopedic, otorhinolaryngologic, brain, and even abdominal surgery departments.

In this study, our unique animal model of PBLI showed that 24-hour survival of mice depended on the magnitude of blast overpressure (from 0.5 bar to 2 bar). With the increase of the peak pressure of shock wave, the mortality rate of mice increased gradually. The research results showed that it could cause severe, sometimes fatal, blast-related acute lung injury when blast overpressure exceed 0.5 bar. Under the condition of 0.5 bar overpressure, all 10 mice survived and exhibited marked lung damage. The injured mice died within 24 hours after the blast or then the mice gradually recovered. Moreover, in the initial stage of blast lung injury, the mice would have symptoms of shortness of breath and even cardiac apnea. Some of the injured mice would bleed in the eyes, ears, mouth, and nasal passages. Our findings are consistent with the characteristics of PBLI reported in previous studies and clinical observation.<sup>15</sup> After simulated blast injury, diffuse small hemorrhagic spots appeared on the lung tissue of mice, especially obviously at 6 hours after injury. Obvious pulmonary edema occurred in the model group, and the highest degree of the edema was found at 6 hours as showed by increased lung coefficient and vascular permeability. Pathological examination of lung tissue showed the ruptured alveolar septal and the infiltration of inflammatory cells in the lung tissue of the injured mice. The recruitment of inflammatory cells in lung tissue indicates the occurrence of inflammatory response in lung tissue from the perspective of pathological injury. The degree of pathological injury of lung tissue reached the peak at 6 hours, and then gradually decreased after 12 hours. Blood cells also appear in the interstitial lung significantly 6 hours after injury, suggesting the occurrence of intrapulmonary hemorrhage.

All these results suggest symptoms of pneumothorax and internal bleeding at this time, which are closely consistent with those seen in clinical patients with PBLI and in laboratory animals in other studies. The reasons for these changes are that the volume of the mouse chest immediately decreased after suffering the blast shock wave and instantly rebounded when the external force was eliminated. During this process, the intrathoracic pressure rises initially and then falls sharply, resulting in the rupture of the alveoli and the pulmonary blood vessels. The permeability of alveoli-capillary membrane increased significantly, and a large number of proteins and cells exude through the blood-gas barrier.<sup>10,15-17</sup> As seen in this study, shock waves induced by our self-made device could cause mice lung damage, which may lead to a variety of pathophysiological changes, including hemorrhage, edema, and inflammatory cells infiltration in the lung.

In this study, the expression of IL-1 $\beta$ , IL-6 and TNF- $\alpha$  in the mice lung tissues was significantly increased in the model group, and peaked within 2 hours and 6 hours, respectively. The expression levels of inflammatory factors in the mice lung tissues were significantly changed only in the earlier acute phase of PBLI, and returned to normal at 24 hours after injury. Combined with pathological observation and molecular level exploration, it was not difficult to find that the lung tissue, as the target organ of the shock wave, occurred obvious inflammatory response. The increase of inflammatory factors in this inflammatory response is positively correlated with the degree of recruitment of inflammatory cells. Inflammatory cells number and recruitment degree are closely related to the degree of lung tissue damage. Previous researches suggested that when lung tissue were damaged by shock waves, the damaged cells released a large number of cytokines, inducing various inflammatory factors.<sup>8,18</sup> Previous studies have reported that PBLI involves an immediate autonomic response, followed by intrapulmonary hemorrhage and histopathological injury, and finally the production of cytokines associated with inflammation.<sup>17</sup> Our findings are basically consistent with the previous results, except that the inflammatory response appears earlier, which is more consistent with the clinical manifestations of critical illness. It indicated that our PBLI animal model could be used in the diagnosis and treatment of PBLI and other related studies in the prehospital phase.

Clinical studies have shown that the initial signs of PBLI are cough, hemoptysis, and other pulmonary symptoms.<sup>19,20</sup> Some of them have hemothorax and/or combined pneumothorax. The victim at the scene of the explosion often have various degrees of visceral injury without significant surface damage, a minority of patients developed rapidly progressive pneumonia leading to acute respiratory distress syndrome. The main cause of death is shock, respiratory failure, septicemia, even acute respiratory distress syndrome. We wondered if there was relationships between hemorrhage, inflammation and other pathological processes in PBLI. How do various pathological processes develop? Is there a key link that connects the various pathologic processes and determines the patient's outcome?

In 2004, Brinkmann et al.<sup>21</sup> reported in *The Journal Science* that neutrophils produce an extracellular fibrous network of DNA, histones, and granulocins, such as elastase, when activated by cytokines or cytotoxins to capture bacteria. This net-

work of extracellular fibers known as NETs, shows significant bactericidal activity. The formation of NETs starts with neutrophil activation followed by ROS production and calcium mobilization. Recently, the role of NETs in the occurrence and development of a variety of bacterial infections or noninfectious diseases has been observed. COVID-19's impact on the respiratory system has gained much attention. Now, reports have been pouring in of the disease's effects throughout the body, many of which are caused by clots.<sup>22</sup> In COVID-19 pneumonia patients, NETs in plasma were found to be significantly higher than those in healthy.<sup>23</sup> Neutrophil extracellular traps play important roles in inflammation and coagulation involved in the development of COVID-19 pneumonia. In addition, Zhang<sup>23</sup> found that NETs mediated systemic changes in blood hypercoagulability in liver ischemia-reperfusion injury and lead to distal organ injury by promoting microvascular immune thrombosis. The role of NETs in PBLI has not been observed in the past studies. In our research, we found that NETs levels in the mice lung tissues peaked at 6 hours after blast injury and recovered over time. That was consistent with inflammatory responses and expression of other injury indicators. These results suggested that NETs maybe involved in PBLI and contribute to the progression of this disease. NETs composition closely matched the trends of inflammatory factors, suggesting that NETs also mediates inflammatory responses in PBLI. However, the specific role of NETs in PBLI mechanism and whether NETs could be a key link between inflammation response and other pathological process in lung after PBLI need further study.

In summary, we induce PBLI in mice successfully by our self-made mini shock tube simulation device. The mice suffered from shock wave have typical lung injury characteristics of PBLI and could be used for PBLI related laboratory study. In the future, studies on the mechanism of PBLI and potential therapeutic or diagnostic approaches at the cellular and molecular levels will be the significant. The study of the role of NETs in PBLI may provide a breakthrough in this area.

#### AUTHORSHIP

J.-F.Z., X.-Y.M. and Q.-Y.L. participated in the literature search. Y.-M.Z., H.-J.F., X.-Y.M., and Q.-Y.L. participated in the study design. X.-Y.M., Q.-Y.L., J.-F.Z., J.-F.L., and M.-Y.S. participated in the data collection. J.-F.Z. and S.-Y.H. participated in the data analysis. J.-F.L., M.-Y.S., and S.-F.Y. participated in the data interpretation. J.-F.Z. participated in the writing. X.-Y.M., Q.-Y.L., Y.-M.Z., and H.-J.F. participated in the critical revision.

#### ACKNOWLEDGMENTS

Availability of data and materials: The data and materials used in the current study are all available from the corresponding author upon reasonable request.

This study was supported by the Open Scientific Research Program of Military Logistics by H.-J.F. (BLB19J006) and Y.-M.Z. (BLB20J009) and the Scientific Research Translational Foundation of Wenzhou Safety (Emergency) Institute of Tianjin University (TJUWY2022002).

#### DISCLOSURE

Ethics approval and consent to participate: The experiments involving animals were approved by the animal care and use ethical committee of Yi Shengyuan Gene Technology (Tianjin) (YSY-DWLL-2021013) and complied with the Guide for the Care and Use of Laboratory Animals approved by the National Institutes of Health. The authors declare no conflicts of interest.

## REFERENCES

1. Yang C, Dong-Hai Z, Ling-Ying L, Yong-Hui Y, Yang W, Li-Wei Z, Rui-Guo H, Jia-Ke C. Simulation of blast lung injury induced by shock waves of five distances based on finite element modeling of a three-dimensional rat. *Sci Rep*. 2019;9(1):3440.
2. Mackenzie IM, Tunnicliffe B. Blast injuries to the lung: epidemiology and management. *Philos Trans R Soc Lond Ser B Biol Sci*. 2011;366(1562):295–299.
3. Lichtenberger JP, Kim AM, Fisher D, Tatum PS, Neubauer B, Peterson PG, Carter BW. Imaging of combat-related thoracic trauma—blunt trauma and blast lung injury. *Mil Med*. 2018;183(3–4):e89–89e96.
4. Wolf SJ, Bebarta VS, Bonnett CJ, Pons PT, Cantrill SV. Blast injuries. *Lancet*. 2009;374(9687):405–415.
5. Smith JE. The epidemiology of blast lung injury during recent military conflicts: a retrospective database review of cases presenting to deployed military hospitals, 2003–2009. *Philos Trans R Soc Lond Ser B Biol Sci*. 2011;366(1562):291–294.
6. Cooper GJ, Townend DJ, Cater SR, Pearce BP. The role of stress waves in thoracic visceral injury from blast loading: modification of stress transmission by foams and high-density materials. *J Biomech*. 1991;24(5):273–285.
7. Cooper GJ, Pearce BP, Sedman AJ, Bush IS, Oakley CW. Experimental evaluation of a rig to simulate the response of the thorax to blast loading. *J Trauma*. 1996;40(Suppl 3):S38–S41.
8. Tong C, Liu Y, Zhang Y, Cong P, Shi X, Liu Y, Lin S, Shi Hongxu Jin L, Hou M. Shock waves increase pulmonary vascular leakage, inflammation, oxidative stress, and apoptosis in a mouse model. *Exp Biol Med (Maywood)*. 2018;243(11):934–944.
9. von Meijenfeldt FA, Stravitz RT, Zhang J, Adelmeijer J, Zen Y, Durkalski V, Lee WM, Lisman T. Generation of neutrophil extracellular traps in patients with acute liver failure is associated with poor outcome. *Hepatology*. 2022;75:623–633.
10. Wu S, Han G, Kang J, Zhang L, Wang A, Wang J. Pulmonary microvascular dysfunction and pathological changes induced by blast injury in a rabbit model. *Ulus Travma Acil Cerrahi Derg*. 2016;22(5):405–411.
11. Zhao Y, Zhou YG. The past and present of blast injury research in China. *Chin J Traumatol*. 2015;18(4):194–200.
12. Yang Z, Aderemi OA, Zhao Q, Edsall PR, Simovic MO, Lund BJ, Espinoza MD, Woodson AM, Li Y, Cancio LC. Early complement and fibrinolytic activation in a rat model of blast-induced multi-organ damage. *Mil Med*. 2019;184(Suppl 1):282–290.
13. Li Y, Yang Z, Chavko M, Liu B, Aderemi OA, Simovic MO, Dubick MA, Cancio LC. Complement inhibition ameliorates blast-induced acute lung injury in rats: potential role of complement in intracellular HMGB1-mediated inflammation. *PLoS One*. 2018;13(8):e0202594.
14. Mishra V, Skotak M, Schuetz H, Heller A, Haorah J, Chandra N. Primary blast causes mild, moderate, severe and lethal TBI with increasing blast overpressures: experimental rat injury model. *Sci Rep*. 2016;6:26992.
15. Scott T, Hulse E, Haque M, Kirkman E, Hardman J, Mahoney P. Modelling primary blast lung injury: current capability and future direction. *J R Army Med Corps*. 2017;163(2):84–88.
16. de Candole CA. Blast injury. *Can Med Assoc J*. 1967;96(4):207–214.
17. Scott TE, Kirkman E, Haque M, Gibb IE, Mahoney P, Hardman JG. Primary blast lung injury—a review. *Br J Anaesth*. 2017;118(3):311–316.
18. Barnett-Vanes A, Sharrock A, Eftaxiopoulou T, Arora H, Macdonald W, Bull AM, Rankin SM. CD43Lo classical monocytes participate in the cellular immune response to isolated primary blast lung injury. *J Trauma Acute Care Surg*. 2016;81(3):500–511.
19. Zhang Y, Meng W, Wang M, Ren W, Wang G, Zhang G, Zhu M. The epidemiological features of blast injury of lungs caused by gas explosion. *Zhonghua Lao Dong Wei Sheng Zhi Ye Bing Za Zhi*. 2012;30(8):582–583.
20. Lee K, Yoon J, Min K, Lee J, Kang S, Hong SJ, Yoon SH, Lee JS, Nam KW, Cho SH, et al. An objective index to estimate the survival rate of primary blast lung injury. *Annu Int Conf IEEE Eng Med Biol Soc*. 2014;2014:1206–1209.
21. Brinkmann V, Reichard U, Goosmann C, Fauler B, Uhlemann Y, Weiss DS, Weinrauch Y, Zychlinsky A. Neutrophil extracellular traps kill bacteria. *Science*. 2004;303(5663):1532–1535.
22. Willyard C. Coronavirus blood-clot mystery intensifies. *Nature*. 2020;581(7808):250.
23. Skendros P, Mitsios A, Chrysanthopoulou A, Mastellos DC, Metallidis S, Rafailidis P, Ntinopoulou M, Sertaridou E, Tsironidou V, Tsigalou C, et al. Complement and tissue factor-enriched neutrophil extracellular traps are key drivers in COVID-19 immunothrombosis. *J Clin Invest*. 2020;130(11):6151–6157.